HHS Public Access

Author manuscript

Pediatr Radiol. Author manuscript; available in PMC 2019 July 01.

Published in final edited form as:

Pediatr Radiol. 2019 January ; 49(1): 57–67. doi:10.1007/s00247-018-4257-y.

4-D flow MRI aortic 3-D hemodynamics and wall shear stress remain stable over short-term follow-up in pediatric and young adult patients with bicuspid aortic valve

Michael J. Rose[1], **Cynthia K. Rigsby**[1,2,3], **Haben Berhane**[1], **Emilie Bollache**[2], **Kelly Jarvis**[2,4], **Alex J. Barker**[2], **Susanne Schnell**[2], **Bradley D. Allen**[2], **Joshua D. Robinson**[2,3,5], and **Michael Markl**[2,4]

[1]Department of Medical Imaging, Ann & Robert H. Lurie Children's Hospital of Chicago, 225 E. Chicago Ave., Chicago, IL 60611, USA

[2]Department of Radiology, Northwestern University Feinberg School of Medicine, Chicago, IL, USA

[3]Department of Pediatrics, Northwestern University Feinberg School of Medicine, Chicago, IL, USA

[4]Biomedical Engineering, Northwestern University, Chicago, IL, USA

[5]Pediatric Cardiology, Ann & Robert H. Lurie Children's Hospital of Chicago, Chicago, IL, USA

Abstract

Background—Children with bicuspid aortic valve (BAV) are at risk for serious complications including aortic valve stenosis and aortic rupture. Most studies investigating biomarkers predictive of BAV complications are focused on adults.

Objective—To investigate whether hemodynamic parameters change over time in children and young adults with BAV by comparing baseline and follow-up four-dimensional (4-D) flow MRI examinations.

Materials and methods—We retrospectively included 19 children and young adults with BAV who had serial 4-D flow MRI exams (mean difference in scan dates 1.8±1.0 [range, 0.6–3.4 years]). We compared aortic peak blood flow velocity, three-dimensional (3-D) wall shear stress, aortic root and ascending aortic (AAo) z-scores between baseline and follow-up exams. We generated systolic streamlines for all patients and visually compared their baseline and follow-up exams.

Results—The only significant difference between baseline and follow-up exams occurred in AAo z-scores (3.12±2.62 vs. 3.59±2.76, $P<0.05$) indicating growth of the AAo out of proportion to somatic growth. There were no significant changes in either peak velocity or 3-D wall shear stress between baseline and follow-up exams. Ascending aortic peak velocity at baseline correlated with annual change in AAo z-score ($r=0.58$, $P=0.009$). Visual assessment revealed

Correspondence to: Cynthia K. Rigsby.

Conflicts of interest None

abnormal blood flow patterns, which were unique to each patient and remained stable between baseline and follow-up exams.

Conclusion—In our pediatric and young adult BAV cohort, hemodynamic markers and systolic blood flow patterns remained stable over short-term follow-up despite significant AAo growth, suggesting minimal acute disease progression. Baseline AAo peak velocity was a predictor of AAo dilation and might help in determining pediatric patients with BAV who are at risk of increased AAo growth.

Keywords

Bicuspid aortic valve; Children; Congenital heart disease; 4-D flow; Heart; Magnetic resonance imaging; Wall shear stress

Introduction

Bicuspid aortic valve (BAV) is the most common congenital cardiac defect, with an estimated prevalence in the general population of 0.5–2% [1]. People with BAV are often asymptomatic in childhood and adolescence but are at risk for serious future complications such as aortic valve stenosis, aortic aneurysm and aortic dissection [2–7]. Researchers have identified valve degeneration and aortic dilation as a prognostic indicators for adverse cardiac events [5, 8, 9] and suggest that people with these findings be followed more frequently. Valve morphology has also been shown to potentially play a role in BAV disease progression [7, 10–13]. Different commissure fusion patterns lead to different transvalvular aortic outflow jet angles and can increase wall shear stress on various areas of the ascending aorta (AAo). Recent developments in four-dimensional (4-D) flow MRI have allowed for the three-dimensional (3-D) quantification of wall shear stress [14] and provide evidence that elevated wall shear stress in people with BAV is associated with BAV morphology, expression of aortic pathology type [15], and aortic medial wall degeneration at histopathology [16].

Most studies investigating biomarkers predictive for BAV complications have focused on adults [9, 10, 15, 17, 18]. Less is known about how the disease progresses in children and adolescents, even though progressive dilation begins in childhood [7, 19, 20]. A study by Holmes et al. [12] found that the pediatric BAV population underwent greatly increased AAo growth rates compared to normal children. Another study found that pediatric patients with BAV with left–right coronary commissure fusion morphology are at increased risk for aortic root dilation and that baseline aortic annular hypoplasia predicts progressive aortic stenosis [21]. However these studies used echocardiographic data and lacked the anatomical measurements and advanced hemodynamic parameters (wall shear stress, 3-D blood flow visualization) available with 4-D flow MRI, and these measurements might provide additional insight into BAV disease progression.

We investigated whether hemodynamic parameters change over time in children and young adults with BAV by comparing baseline and follow-up aortic size, peak aortic velocities, aortic 3-D wall shear stress, and systolic flow patterns on serial MRI examinations.

Materials and methods

Patient selection and characteristics

Twenty-five children and young adults with BAV who received baseline and at least one follow-up 4-D flow MRI study performed as part of a physician-ordered cardiac MRI were included in this retrospective study. We obtained institutional review board (IRB) approval and complied with the Health Insurance Portability and Accountability Act. Consent was obtained for 4-D flow MRI per IRB protocol. In the case of children with multiple follow-ups, we analyzed all follow-ups but only considered the most recent follow-up in comparative analysis with the baseline study. Exclusion criteria included aortic valve replacement, surgical intervention between baseline and follow-up, complex congenital heart disease, and any connective tissue disease other than Turner syndrome. Patients were anesthetized for MRI studies according to institutional protocol. To investigate whether specific subgroups of people with BAV underwent different rates and mechanisms of BAV disease progression, we analyzed patients according to valve morphology. We divided patients into two groups: right–left and right–noncoronary commissure BAV fusion per the Sievers classification [22].

Magnetic resonance imaging

Cardiac MRI studies were performed at 1.5 T (Avanto or Aera; Siemens, Erlangen, Germany) using either a 12-channel body matrix coil (Avanto) or an 18-channel body matrix coil (Aera) on larger patients, or a 4-channel flex coil on smaller patients. Cine steady-state free precession (SSFP) images were obtained in 2- and 4-chamber and short-axis views. Short- and long-axis cine SSFP and/or gradient echo aortic valve and sinus were obtained. Three-dimensional gradient echo MR angiography using respiratory navigator triggering and electrocardiographic (ECG) gating to systole with 1.0–1.5 × 1.0–1.5-mm pixel size and 0.9–1.5-mm slice thickness was performed following administration of contrast agent (gadopentetate dimeglumine/Magnevist by Bayer Healthcare, Berlin, Germany; or gadofosveset trisodium/Ablavar by Lantheus, North Billerica, MA). Four-dimensional flow MRI data were acquired in a 3-D volume set encompassing the thorax with three-directional velocity encoding, respiratory navigator triggering and prospective ECG gating [23]. Four-dimensional flow MRI parameters included: field of view = 180–320 × 135–244 mm^2, matrix = 128–160 × 72–130, spatial resolution = 1.2–3.5 × 1.1–2.5 × 1.2–3.2 mm^3, temporal resolution = 37.6–44.0 ms, echo time/repetition time (TE/TR)/flip angle = 2.3–2.8 ms/4.7–5.3 ms/15° and velocity sensitivity (VENC) = 120–400 cm/s.

Data analysis — aortic dimensions

We used EchoIMS (Merge Healthcare, Chicago, IL) to record aortic root and AAo z-scores from either the systolic 3-D MR angiographic images reconstructed in the axial plane relative to the aortic root or the systolic-phase SSFP or gradient-echo cine images acquired in the axial plane relative to the aortic root. Aortic root measurements were made at the sinuses of Valsalva using the sinus-to-sinus dimension while AAo measurements were made at the largest cross-section of the AAo.

Data analysis — 4-D flow magnetic resonance imaging

Four-dimensional flow MRI data were preprocessed to correct for noise, eddy currents, Maxwell terms and velocity aliasing using an in-house tool [24] (MATLAB; MathWorks, Natick, MA). We computed a time-averaged 3-D phase-contrast angiogram as described previously [23] and used this as an anatomical guide for thoracic aorta 3-D segmentation (Mimics; Materialise, Leuven, Belgium). We used the 3-D segmented aorta to mask the 4-D flow velocity field to further assess blood flow patterns, peak velocity, regurgitant fractions and wall shear stress.

Three-dimensional flow visualization

We generated systolic 3-D streamlines peak systolic time points (EnSight; CEI, Apex, NC) for each scan to visually compare flow patterns throughout the aorta between baseline and follow-up (Fig. 1). For each patient, two observers gave a qualitative consensus score of 0–2; the observers included a pediatric radiologist (C.K.R., with 18 years of cardiovascular MR experience) and a pediatric cardiologist (J.D.R., with 10 years of cardiovascular MR experience) who were blinded to patient history as to whether the patient experienced no change (0), mild change (1) or severe change (2) in blood flow patterns between baseline and most distant follow-up. Grade 1 was defined as a qualitatively mild change in the character of the flow signature, including either an increase or decrease in a vortex or helix pattern, or a change from laminar to helical or vortical flow. Grade 2 was defined as a qualitatively significant change in the character of the flow signature including either an increase or decrease in a vortex or helix pattern, or a change from laminar to helical or vortical flow.

Prior to performing the blinded qualitative assessment, the two readers evaluated five aortic flow studies on subjects who were not included in this study as training data. Because the assessment of change was qualitative, mild versus severe differences in flow patterns were deemed to be definable as a qualitative measure of change. A moderate change could not be qualitatively defined, so a moderate change category was not used. Additionally, to determine whether children with BAV exhibit similar flow patterns to one other or patient-specific flow patterns (flow “signatures”), both observers independently attempted to pair the baseline and follow-up studies presented blindly in a random order as peak systolic streamlines in an oblique sagittal reconstruction. There was at least 1 month of time between the blinded review of the findings for qualitative changes in flow patterns and the blinded attempt to pair the examinations, to avoid recall bias.

Peak velocity calculation, aortic stenosis and aortic regurgitation assessment

We used the masked aorta velocity field to generate peak systolic velocity maximum-intensity projections (MIP) as previously described [25]. Peak systole was defined as the time-point in which the average velocity was highest throughout every voxel in the segment. Peak velocities were extracted from three regions of interest (ROI): the AAo, aortic arch and descending aorta (Fig. 1). The AAo region of interest was defined as beginning immediately below the aortic valve and ending directly proximal to the brachiocephalic trunk. The aortic arch ROI was defined as beginning at the brachiocephalic trunk and ending just distal to the left subclavian artery. The descending aorta ROI was defined as beginning distal to the left

subclavian artery and ending in the mid-descending aorta at the level below the aortic valve. As per American College of Cardiology/American Heart Association guidelines [26], AAo peak velocity less than 2.0 m/s was considered as no stenosis, peak velocity greater than 2.0 m/s and less than 3.0 m/s was considered mild stenosis, peak velocity greater than 3.0 m/s and less than 4.0 m/s was considered moderate stenosis, and peak velocity greater than 4.0 m/s was considered severe stenosis. Mild aortic regurgitation was defined as an aortic valve regurgitant fraction between 5 and 30%. Moderate aortic regurgitation was defined as 30 to 50%. Severe aortic regurgitation was defined as greater than 50%.

Three-dimensional wall shear stress calculations

We used the masked aorta velocity field to calculate peak systolic 3-D wall shear stress vectors along the entire aortic surface as described previously [14] (Fig. 1). Average systolic wall shear stress magnitude was calculated from four ROIs: inner proximal AAo, outer proximal AAo, inner distal AAo and outer distal AAo. The proximal AAo was defined as beginning at the aortic root and ending half-way between the aortic root and brachiocephalic trunk. The distal AAo was defined as half-way between the aortic root and brachiocephalic trunk and ending at the brachiocephalic trunk. The inner AAo was defined as spanning from the inner curvature of the AAo to the centerline of the aorta as viewed on sagittal images. The outer AAo was defined as spanning from the outer curvature of the AAo to the centerline of the aorta as viewed on sagittal images. The boundaries of the ROIs are shown in Fig. 1. Additionally, we calculated the wall shear stress for the entire AAo by averaging across all four ROIs.

Subgroup analysis

We compared baseline and follow-up z-scores, peak velocities and 3-D wall shear stress values for the subgroups of Turner syndrome, right–left commissure and right–noncommissure aortic valve fusion patterns.

Statistical analysis

Continuous variables were provided as means ± standard deviations. The Wilcoxon signed rank test was used to test the significance of the differences between baseline and follow-up of peak velocity, regional mean 3-D wall shear stress, and total average 3-D wall shear stress and aortic root and AAo z-scores. A power calculation based on total subjects and the standard deviations of wall shear stress and peak velocity values was performed to determine the power to detect differences in these values between the baseline and follow-up studies. Pearson correlation coefficients were calculated to test the correlation of relationships between various combinations of root and AAo z-scores and AAo diameter indexed to body surface area, peak velocity, 3-D wall shear stress and age. A P value <0.05 was considered statistically significant.

Results

Patient demographics

Final cohort size was 19 patients with mean age of 14.0 years (standard deviation [SD]±5.7 years; range, 0.9–21.4 years) at baseline, and mean age of 15.7 years (SD±5.6 years; range,

2.0–22.4 years) at follow-up, with a male-to-female ratio of 12:7. Six patients were excluded because of coarctation repair between baseline and follow-up (n=1), interrupted aortic arch repair (n=1), severe velocity aliasing on 4-D flow images (n=1), aortic valve replacement (n=1), substantial metallic artifact (n=1) and Loeys–Dietz syndrome (n=1). Mean±SD time difference between baseline and follow-up was 1.8±1.0 years (range, 0.6–3.4 years). Five patients had right–noncoronary commissure fusion and 14 patients had right–left commissure fusion. Four patients had Turner syndrome but no other patients had connective tissue diseases. Nine patients were taking no cardiac medications at baseline or follow-up, six were taking one cardiac medication at baseline and follow-up (3 lisinopril, 2 atenolol, 1 losartan) and four began taking a cardiac medication between the first and second exams (1 atenolol, 3 losartan; Table 1). Five of 19 patients underwent anesthesia for baseline and follow-up scans; 5 underwent anesthesia for baseline but not for follow-up scans; and 9 did not undergo anesthesia.

Aortic root and ascending aorta z-scores

Aortic z-score results are summarized in Table 2. Aortic root and ascending aortic z-scores were similar for baseline and follow-up (aortic root: 3.25±1.81 vs. 3.45±1.91, P=0.44, mean annual change = 0.2±0.6 per year; AAo: 3.12±2.62 vs. 3.59±2.76, P=0.08, mean annual change = 0.6±0.6 per year).

Three-dimensional flow visualization

Examples of aortic blood flow visualization at baseline and follow-up for six individual patients are shown in Fig. 2. Both observers found 5 patients to have undergone mild changes (grade 1) in blood flow patterns and the remaining 14 patients to have stable 3-D flow patterns between baseline and follow-up (grade 0). One observer successfully paired the baseline and follow-up 3-D streamlines for all 19 patients, while the other observer successfully paired 17 patients, indicating stable signature blood flow characteristics (vortices, helices and flow velocities of similar magnitude and in the same locations) that could easily be discerned at both baseline and follow-up.

Peak velocity, aortic stenosis and aortic regurgitation

Peak systolic velocity results are summarized in Table 2 and Fig. 3. There were no significant changes in peak systolic velocity in any aortic regions for the full cohort or for any of the subgroups. Based on the standard deviations of the peak systolic velocities and a sample size of 19 subjects, this study was determined to have a power of 81% to detect a difference in velocity of 0.6 m/s between baseline and follow-up at P=0.05 significance level. At baseline (Table 1), no aortic stenosis was found in seven patients, mild stenosis was found in nine patients, moderate stenosis was found in two patients and severe stenosis was found in one patient. At follow-up, there was no stenosis in seven patients, mild stenosis in nine patients, moderate stenosis in three patients, and no severe stenosis. The patient who qualified as having severe stenosis at baseline, which then regressed to moderate at follow-up, was borderline between moderate and severe and showed a difference in peak velocity (4.0 m/s vs. 3.9 m/s) that was clinically insignificant and likely indicative of measurement error rather than disease change. One patient had mild aortic regurgitation (regurgitant fraction of 10%) and none had moderate or severe aortic regurgitation.

Three-dimensional wall shear stress

Results of 3-D wall shear stress quantification are summarized in Table 2 and Fig. 3. There were no significant regional changes in 3-D wall shear stress for the full cohort, the Turner subgroup, the right–left commissure fusion subgroup or the right–noncommissure fusion subgroup. For the full cohort, the most pronounced, but non-significant, change in 3-D wall shear stress occurred in the outer proximal aorta (−0.07±0.20 Pa, P=0.12). Based on the standard deviations of wall shear stress and a sample size of 19 subjects, this study was determined to have a power of 85% to detect a difference of 0.25 Pa between baseline and follow-up wall shear stress at P=0.05 significance level.

Correlations

Results of correlation analyses are summarized in Table 3. There was a significant relationship between baseline peak AAo velocity and AAo z-score change per year (r=0.57, P=0.01) and annual change in AAo z-score between baseline and follow-up (r=0.58, P=0.01; Fig. 4). There was no significant correlation between baseline wall shear stress and aortic diameters indexed to body surface area (r=−0.25, P=0.32).

Subgroup analysis

Results for the Turner syndrome, right–left commissure and right–noncommissure fusion pattern subgroup analyses are summarized in Table 2. There were no significant changes between baseline and follow-up for any of the parameters evaluated.

Discussion

Our findings illustrate the stability of 3-D wall shear stress and peak velocity in our cohort of children and young adults with BAV, with no significant changes in these parameters during a mean follow-up time of 1.8±1.0 years. Our visual assessment of systolic streamlines revealed unique, patient-specific flow derangement patterns that remained relatively unchanged over time.

A prior study investigating the test–retest stability of thoracic 4-D flow parameters in 14 healthy adult controls who underwent test–retest aortic 4-D flow MRI studies separated by 16±3 days showed that systolic velocity and wall shear stress derived from 4-D flow MRI are reproducible between consecutive visits with low inter-observer variability [27]. Our study adds to the 4-D flow MRI stability literature in that our BAV patients had stable flow parameters over a longer period of follow-up time than this prior study’s test–retest evaluation period.

We also found a significant correlation between elevated AAo peak velocity at baseline and AAo diameter growth between baseline and follow-up exams. The relationship between baseline AAo peak velocity and AAo diameter growth suggests that elevated peak velocity is predictive of AAo dilation in subjects with BAV. Bissel et al. [10] found that people with BAV and with aortic stenosis had increased mid AAo diameters compared to those without stenosis. However their study did not assess longitudinal data. A long-term follow-up study of 416 adults with BAV by Michelena et al. [3] found baseline aortic stenosis to be a

predictor of aortic aneurysm formation. Their findings are in line with ours and suggest that elevated peak velocity might predict AAo growth.

We also found there were significant increases in AAo z-scores between baseline and follow-up for our entire cohort. Our findings indicate that our cohort underwent aortic growth out of proportion to somatic growth and at an increased rate relative to the general pediatric population, which is in accordance with adult and pediatric data [12, 17].

Our results showed no significant correlation between baseline 3-D wall shear stress and aortic diameters. This is contrary to what has been reported in adults with BAV, where increased wall shear stress has been found to correlate with increased AAo diameters and in adults with aortic aneurysm [10] where increased wall shear stress has been found to be significantly lower in the dilated AAo [28]. In our study, we measured AAo z-scores instead of absolute AAo diameters, which might make our detection of diameter changes less sensitive and result in missing the correlation between wall shear stress and AAo dilation. Additionally, our short-term follow-up might not provide sufficient time for interval wall shear stress change. Wall shear stress and peak velocity stability between scans suggests little disease progression over the time period studied. The stability highlights the reproducibility of 4-D flow 3-D wall shear stress and peak velocity measurements. A previous study investigated hemodynamics (3-D wall shear stress, peak velocity and aortic z-scores) using 4-D flow MRI in 30 children and young adults with BAV [29]. Like us, those authors found no correlation between wall shear stress and AAo z-scores. However, unlike in our study, they found no correlation between peak velocity and AAo z-scores. The disagreement might be explained by differences in study design because we used longitudinal data while their study was limited to a single exam per patient.

The importance of identifying patient-specific changes for surveillance is further supported by our visual analysis of systolic 3-D streamlines. We found that patients had unique flow signatures that remained stable over time. We also found stable hemodynamics, with stable peak velocity and 3-D wall shear stress despite significant AAo growth. This suggests no substantial short-term disease progression. It is beyond the scope of the study to explain the variance of flow patterns among patients, but recent studies have reported valve morphology and flow jet angle to be primary drivers of blood flow patterns in the presence of BAV [10, 30]. Future more quantitative analysis using artificial intelligence might prove useful for flow pattern grading.

Our study has limitations. The main limitation is the short-term follow-up, so it is possible that we did not observe significant changes in 3-D wall shear stress and peak velocity because of insufficient time between exams. We are also limited by the retrospective nature of our study of people with BAV referred for two MRI exams during our data collection timeframe, so it is possible that these patients have greater disease severity than the general BAV population and the results might by skewed by selection bias. Our cohort was relatively small, so because of the scarcity of longitudinal pediatric and young adult BAV 4-D flow data, we were conservative with exclusion criteria and included those with surgical or catheter interventions if the native aortic valve was spared and the surgical intervention did not occur between baseline and follow-up scans. This introduces confounding factors and

results in a heterogeneous cohort of children and young adults with BAV who might not represent the general BAV population. Additionally, the small study cohort resulted in even smaller subgroups for analysis based on valve morphology and Turner syndrome. The lack of significant results in the velocity and wall shear stress analyses could be a result of small sample size; however the power calculations suggest that we would have seen any clinically significant differences in velocity (power of 81% to detect a difference in velocity of 0.6 m/s between baseline and follow-up at P=0.05 significance level) and significant differences in wall shear stress (power of 85% to detect a difference of 0.25 Pa between baseline and follow-up at a P=0.05 significance level). Ten patients received anesthesia for the examination, so comparison of these examinations with those not performed under anesthesia might be compromised because of the reported anesthetic effects on cardiac output [31]. Last, 6 of the 19 patients in our cohort were taking cardiac medications prior to the baseline scan and 4 of the 19 patients began taking a cardiac medication between the baseline and the first follow-up examination. How these medications might have affected aortic growth rates in this small population is not known.

Conclusion

Children and young adults with BAV undergo increased AAo growth rates compared with healthy controls and might be at higher risk for aortic dilation if they have elevated baseline AAo peak velocities. Additionally, peak velocity, 3-D wall shear stress and signature systolic 3-D blood flow patterns remain stable over short-term follow-up even if there is significant AAo growth. Four-dimensional flow MRI might be useful in monitoring people with BAV by providing noninvasive and robust quantitative measures of the entire thoracic aorta along with 3-D blood flow visualization. Longer-term follow-up is needed to further understand how pediatric and young adult BAV disease progresses and which patients are at increased risk for adverse cardiovascular events.

Acknowledgments

We thank Marci Messina, RT(R)(MR), for scanning and Ryan Kuhn, Sebastian Garcia and Paige Nelson for data collection and patient consent. This work was supported by National Institutes of Health grants R01 HL115828 and K25 HL119608, and American Heart Association Midwest Affiliate grants 6POST27250158 and 16SDG30420005.

References

1. Siu SC, Silversides CK (2010) Bicuspid aortic valve disease. J Am Coll Cardiol 55:2789–2800 [PubMed: 20579534]
2. Subramanian R, Olson LJ, Edwards WD (1984) Surgical pathology of pure aortic stenosis: a study of 374 cases. Mayo Clin Proc 59:683–690 [PubMed: 6482513]
3. Michelena HI, Khanna AD, Mahoney D et al. (2011) Incidence of aortic complications in patients with bicuspid aortic valves. JAMA 306:1104–1112 [PubMed: 21917581]
4. Sabet HY, Edwards WD, Tazelaar HD et al. (1999) Congenitally bicuspid aortic valves: a surgical pathology study of 542 cases (1991 through 1996) and a literature review of 2,715 additional cases. Mayo Clin Proc 74:14–26 [PubMed: 9987528]
5. Larson EW, Edwards WD (1984) Risk factors for aortic dissection: a necropsy study of 161 cases. Am J Cardiol 53:849–855 [PubMed: 6702637]
6. Roberts CS, Roberts WC (1991) Dissection of the aorta associated with congenital malformation of the aortic valve. J Am Coll Cardiol 17:712–716 [PubMed: 1993792]

7. Verma S, Siu SC (2014) Aortic dilatation in patients with bicuspid aortic valve. N Engl J Med 370:1920–1929 [PubMed: 24827036]
8. Ward C (2000) Clinical significance of the bicuspid aortic valve. Heart 83:81–85 [PubMed: 10618341]
9. Michelena HI, Desjardins VA, Avierinos JF et al. (2008) Natural history of asymptomatic patients with normally functioning or minimally dysfunctional bicuspid aortic valve in the community. Circulation 117:2776–2784 [PubMed: 18506017]
10. Bissell MM, Hess AT, Biasiolli L et al. (2013) Aortic dilation in bicuspid aortic valve disease: flow pattern is a major contributor and differs with valve fusion type. Circ Cardiovasc Imaging 6:499–507 [PubMed: 23771987]
11. Girdauskas E, Disha K, Borger MA et al. (2012) Relation of bicuspid aortic valve morphology to the dilatation pattern of the proximal aorta: focus on the transvalvular flow. Cardiol Res Pract 2012:478259 [PubMed: 22900225]
12. Holmes KW, Lehmann CU, Dalal D et al. (2007) Progressive dilation of the ascending aorta in children with isolated bicuspid aortic valve. Am J Cardiol 99:978–983 [PubMed: 17398196]
13. Pees C, Michel-Behnke I (2012) Morphology of the bicuspid aortic valve and elasticity of the adjacent aorta in children. Am J Cardiol 110:1354–1360 [PubMed: 22819430]
14. Potters WV, van Ooij P, Marquering H et al. (2015) Volumetric arterial wall shear stress calculation based on cine phase contrast MRI. J Magn Reson Imaging 41:505–516 [PubMed: 24436246]
15. Mahadevia R, Barker AJ, Schnell S et al. (2014) Bicuspid aortic cusp fusion morphology alters aortic three-dimensional outflow patterns, wall shear stress, and expression of aortopathy. Circulation 129:673–682 [PubMed: 24345403]
16. Guzzardi DG, Barker AJ, van Ooij P et al. (2015) Valve-related hemodynamics mediate human bicuspid aortopathy: insights from wall shear stress mapping. J Am Coll Cardiol 66:892–900 [PubMed: 26293758]
17. Dore A, Brochu MC, Baril JF et al. (2003) Progressive dilation of the diameter of the aortic root in adults with a bicuspid aortic valve. Cardiol Young 13:526–531 [PubMed: 14982293]
18. Ferencik M, Pape LA (2003) Changes in size of ascending aorta and aortic valve function with time in patients with congenitally bicuspid aortic valves. Am J Cardiol 92:43–46 [PubMed: 12842243]
19. Nistri S, Sorbo MD, Marin M et al. (1999) Aortic root dilatation in young men with normally functioning bicuspid aortic valves. Heart 82:19–22 [PubMed: 10377302]
20. Warren AE, Boyd ML, O'Connell C et al. (2006) Dilatation of the ascending aorta in paediatric patients with bicuspid aortic valve: frequency, rate of progression and risk factors. Heart 92:1496–1500 [PubMed: 16547208]
21. Spaziani G, Ballo P, Favilli S et al. (2014) Clinical outcome, valve dysfunction, and progressive aortic dilation in a pediatric population with isolated bicuspid aortic valve. Pediatr Cardiol 35:803–809 [PubMed: 24362596]
22. Sievers HH, Schmidtke C (2007) A classification system for the bicuspid aortic valve from 304 surgical specimens. J Thorac Cardiovasc Surg 133:1226–1233 [PubMed: 17467434]
23. Markl M, Harloff A, Bley TA et al. (2007) Time-resolved 3D MR velocity mapping at 3T: improved navigator-gated assessment of vascular anatomy and blood flow. J Magn Reson Imaging 25:824–831 [PubMed: 17345635]
24. Bock J, Kreher B, Hennig J, Markl M (2007) Optimized preprocessing of time-resolved 2D and 3D phase contrast MRI data The 15th annual meeting of ISMRM, Berlin, Germany
25. Rose MJ, Jarvis K, Chowdhary V et al. (2016) Efficient method for volumetric assessment of peak blood flow velocity using 4D flow MRI. J Magn Reson Imaging 44:1673–1682 [PubMed: 27192153]
26. Nishimura RA, Otto CM, Bonow RO et al. (2014) 2014 AHA/ACC guideline for the management of patients with valvular heart disease: executive summary: a report of the American College of Cardiology/American Heart Association task force on practice guidelines. J Am Coll Cardiol 63:2438–2488 [PubMed: 24603192]

27. van Ooij P, Powell AL, Potters WVet al (2016) Reproducibility and interobserver variability of systolic blood flow velocity and 3D wall shear stress derived from 4D flow MRI in the healthy aorta. J Magn Reson Imaging 43:236–248 [PubMed: 26140480]

28. Burk J, Blanke P, Stankovic Z et al. (2012) Evaluation of 3D blood flow patterns and wall shear stress in the normal and dilated thoracic aorta using flow-sensitive 4D CMR. J Cardiovasc Magn Reson 14: 84 [PubMed: 23237187]

29. Allen BD, van Ooij P, Barker AJ et al. (2015) Thoracic aorta 3D hemodynamics in pediatric and young adult patients with bicuspid aortic valve. J Magn Reson Imaging 42:954–963 [PubMed: 25644073]

30. Hope MD, Hope TA, Meadows AK et al. (2010) Bicuspid aortic valve: four-dimensional MR evaluation of ascending aortic systolic flow patterns. Radiology 255:53–61 [PubMed: 20308444]

31. De Hert SG (2006) Volatile anesthetics and cardiac function. Semin Cardiothorac Vasc Anesth 10:33–42 [PubMed: 16703232]

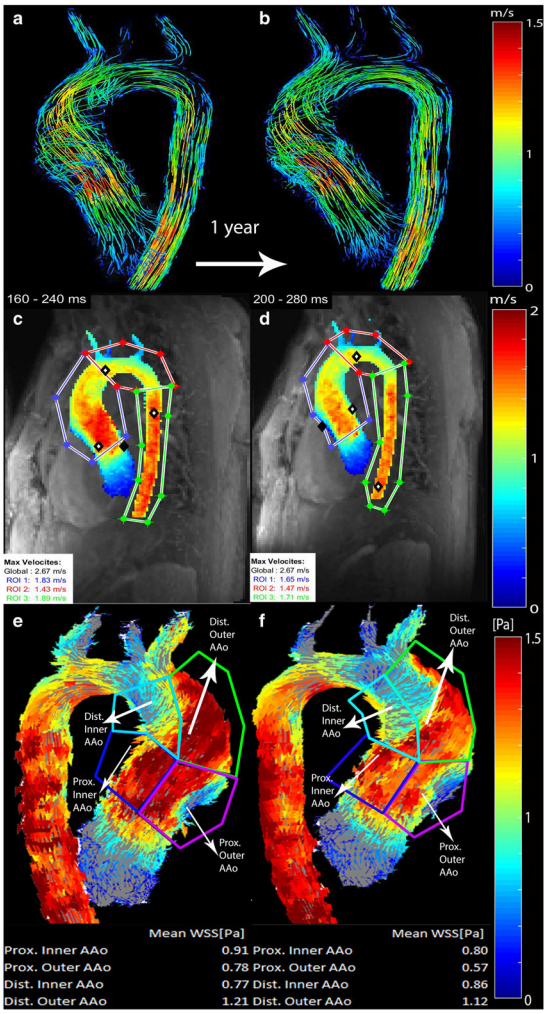

◀Fig. 1.

Comparison of baseline (**a**, **c**, **e**; 16.7 years old) and follow-up (**b**, **d**, **f**; 17.7 years old) scans for a boy with bicuspid aortic valve with right–left commissure fusion pattern. Systolic 3-D streamline flow patterns color-coded by velocity (in m/s) at different time points. **a, b** Peak systolic velocities were extracted from velocity maximum-intensity projections (**c, d**) in the ascending aorta, (*AAo*) arch, and descending aorta. Regional wall shear stress (*WSS*) values (in pascals, or Pa) were calculated from wall shear stress maps (**e, f**) for inner proximal, outer proximal, inner distal and outer distal ascending aortic regions

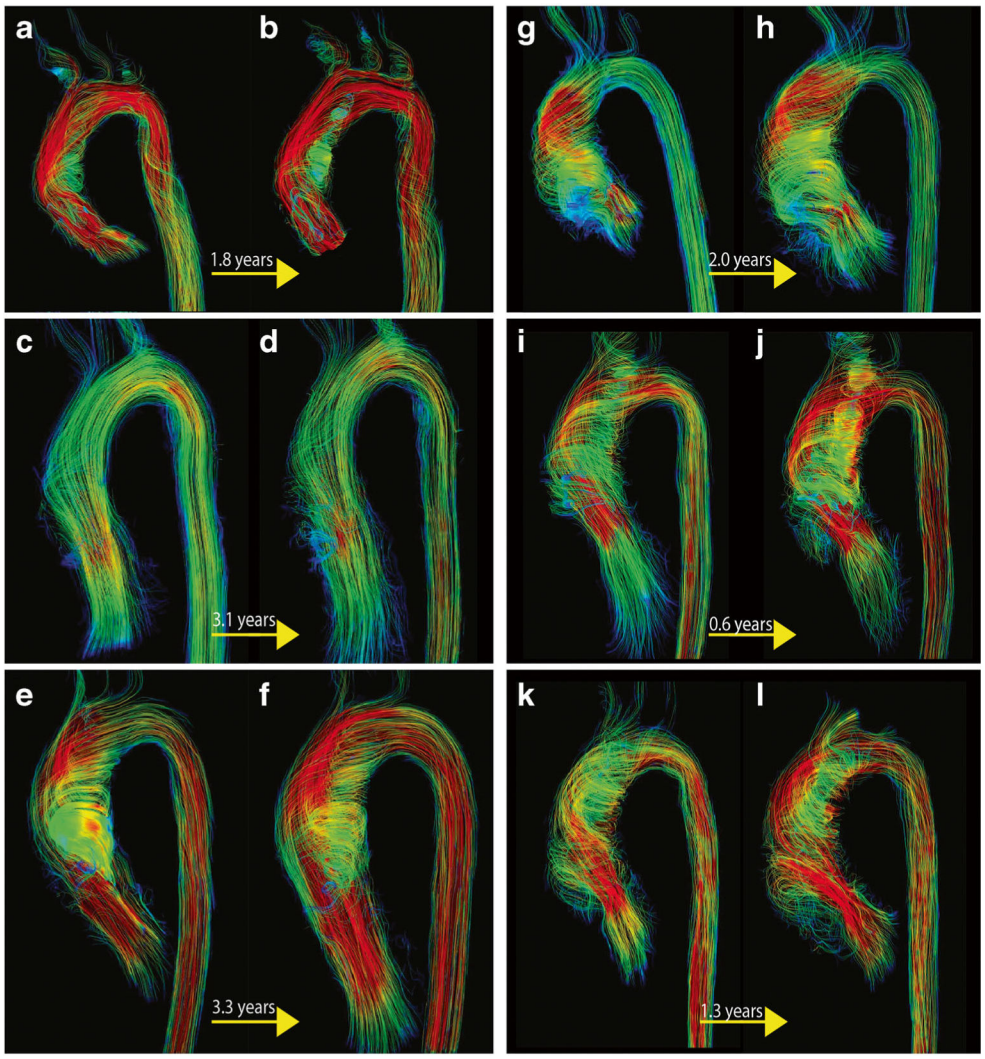

Fig. 2.

Systolic 3-D streamlines color-coded by velocity of baseline (*left*) and follow-up (*right*) scans for six subjects with bicuspid aortic valve showcase the similar signature flow patterns for each patient over time. Except for one patient (panel **c, d**), all demonstrate deranged flow patterns. Panel **a, b**: Patient 4. Female with right–left commissure fusion pattern shows marked helix flow in the ascending aorta (AAo) and increased systolic velocity (*red* = velocity greater than 1.8 m/s) present at baseline (19.9 years old; **a**) and follow-up (21.7 years old; **b**). Panel **c, d**: Patient 3. Male with right–left commissure fusion pattern and normal cohesive 3-D streamlines with mildly increased aortic root and arch velocity at baseline (11.3 years old; **c**) and follow-up (14.4 years old; **d**). Panel **e, f**: Patient 17. Male with right–left commissure fusion pattern and pronounced AAo helix flow and elevated aortic velocity at baseline (13.0 years old; **e**) and follow-up (16.3 years old; **f**). Panel **g, h**: Patient 16. Female with right–noncommissure fusion pattern and pronounced helix proximal AAo flow that tapers off in the distal AAo, at baseline (8.0 years old; **g**) and follow-up (10.0 years old; **h**). Panel **i, j**: Patient 15. Female with right–noncommissure fusion pattern and a tightly wound helix in the AAo at baseline (10.2 years old; **i**) and follow-up (10.8 years old;

j). Panel **k, l**: Patient 10. Male with right–left commissure fusion pattern and high-velocity aortic root and helix flow throughout the AAo at baseline (4.4 years old; **k**) and follow-up (5.7 years old; **l**). One observer matched all baseline and follow-up patient images and one observer was only unable to match images (**k**) and (**l**) as the same patient

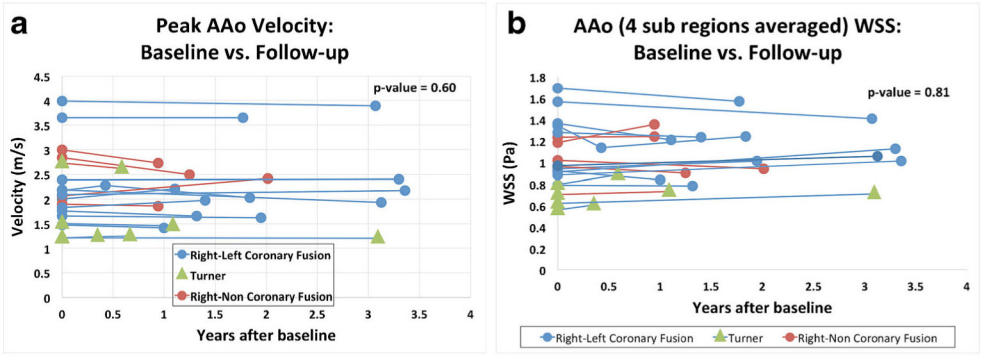

Fig. 3.

Differences in velocity (**a**) and wall shear stress (WSS; **b**) in the ascending aorta (AAo) between baseline and follow-up for each patient

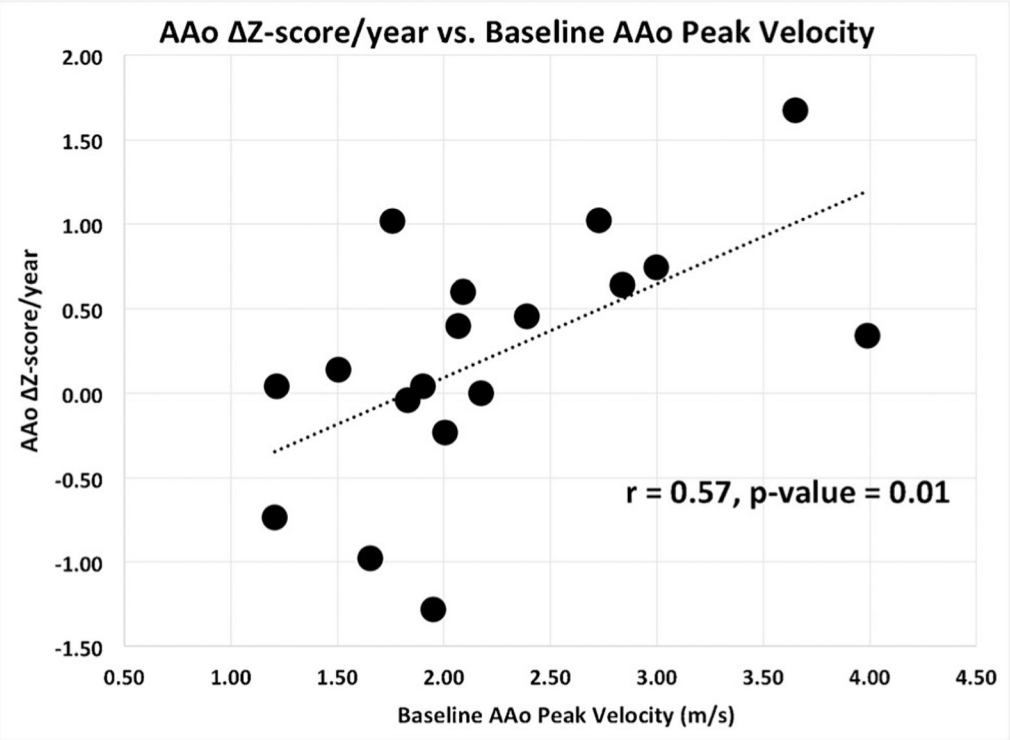

Fig. 4.

Change in ascending aortic (AAo) z-score per year vs. baseline AAo peak velocity for all patients. The outlier data likely reflect the imperfect correlation between the change in AAo z-score and baseline peak velocity in this small cohort

Table 1

Individual patient information

Patient number	Commissure fusion pattern	Other diagnoses	Surgical or Interventional procedure(s)	Age at first scan, years	Aortic root dimension z-score at first scan	Medication	Aortic stenosis (mild, moderate, severe)	Aortic regurgitation (mild, moderate, severe)	Mean ascending aortic wall shear stress at first scan, Pa
1	R/L fusion			16.7	0.6	None	Mild		0.94
2	R/L fusion	Turner		12.1	2.1	None			0.62
3	R/L fusion		Balloon valvotomy	11.3	3.7	None	Severe		1.57
4	R/L fusion	Coarctation of the aorta, ASD, PAPVR	Coarctation repair, ASD closure, repair of PAPVR	19.9	1.6	Lisinopril prior to first scan	Moderate		1.69
5	R/L fusion	Turner, PAPVR		14.4	6.0	Atenolol between scans			0.56
6	R/L fusion	Mildly hypoplastic arch and mitral valve		0.9	1.0	None	Mild		1.36
7	R/N fusion			18.8	3.4	Losartan between scans	Mild		0.96
8	R/N fusion			17.4	5.3	Atenolol prior to first scan	Moderate		1.23
9	R/L fusion	Coarctation of the aorta	Coarctation repair	19.7	4.3	Losartan between scans	Mild		1.34
10	R/L fusion			4.4	6.0	None			0.79
12	R/L fusion			14.1	4.3	Atenolol prior to first scan			0.94
12	R/N fusion	Coarctation of the aorta	Coarctation repair	21.4	1.3	None			1.18
13	R/L fusion	Turner, coarctation of the aorta	Coarctation repair	20.1	3.3	Lisinopril prior to first scan		Mild	0.70
14	R/L fusion	Coarctation of the aorta	Coarctation repair	16.6	1.4	Lisinopril prior to first scan			1.28
15	R/N fusion	Turner	Balloon aortic valvuloplasty	10.2	4.7	Losartan prior to first scan	Mild		0.79
16	R/N fusion			8.0	5.1	Losartan between scans	Mild		1.02
17	R/L fusion			13.0	16.3	None	Mild		0.42
18	R/L fusion			13.3	16.4	None	Mild		0.97
19	R/L fusion			14.1	17.4	None	Mild		0.88

ASD atrial septal defect, *Pa* pascal, *PAPVR* partial anomalous pulmonary venous return, *R/L fusion* right–left commissure fusion pattern, *R/N fusion* right–noncommissure fusion pattern, *Turner* Turner syndrome, *VSD* ventricular septal defect

Table 2

Patient demographics, hemodynamic and z-score values for the full cohort, Turner syndrome sub-cohort, right–left commissure and right–noncommissure fusion pattern sub-cohorts

	Full cohort			**Turner syndrome**			**Right-left commissure fusion**			**Right-noncommissure fusion**		
	Baseline	**Follow-up**	***P* value**	**Baseline**	**Follow-up**	***P* value**	**Baseline**	**Follow-up**	***P* value**	**Baseline**	**Follow-up**	***P* value**
n	19	19		4	4		14	14		5	5	
M:F	12:7	12:7		0:4	0:4		9:5	9:5		3:2	3:2	
Age (years)	14.0 ± 5.8	15.7 ± 5.6		14.2 ± 4.3	15.6 ± 4.3		13.1 ± 5.6	15.1 ± 5.7		15.1 ± 5.8	16.6 ± 5.9	
Root z-score	3.25 ± 1.81	3.45 ± 1.91	0.44	4.03 ± 1.66	4.10 ± 1.94	0.50	3.00 ± 1.78	3.17 ± 1.83	0.46	3.98 ± 1.68	4.07 ± 1.97	0.81
AAo z-score	**3.12 ± 2.62**	**3.59 ± 2.76**	**0.08**	2.92 ± 1.89	3.01 ± 2.02	0.63	2.99 ± 2.56	3.43 ± 2.76	0.27	3.45 ± 2.77	4.04 ± 3.02	0.06
AAo peak velocity (m/s)	2.21 ± 0.75	2.17 ± 0.72	0.23	1.66 ± 0.72	1.63 ± 0.67	0.38	2.11 ± 0.81	2.08 ± 0.80	0.43	2.51 ± 0.49	2.42 ± 0.34	0.63
Arch peak velocity (m/s)	1.62 ± 0.42	1.64 ± 0.40	0.69	1.32 ± 0.42	1.63 ± 0.33	0.63	1.59 ± 0.45	1.63 ± 0.45	0.27	1.72 ± 0.27	1.65 ± 0.23	0.44
DAo peak velocity (m/s)	1.51 ± 0.36	1.53 ± 0.29	0.57	1.28 ± 0.32	1.35 ± 0.21	0.63	1.46 ± 0.37	1.54 ± 0.33	0.12	1.64 ± 0.32	1.51 ± 0.18	0.44
Inner prox AAo WSS (Pa)	0.94 ± 0.22	0.97 ± 0.22	0.18	0.69 ± 0.09	0.72 ± 0.11	0.63	0.92 ± 0.24	0.95 ± 0.23	0.30	0.98 ± 0.18	1.03 ± 0.21	0.63
Outer prox AAo WSS (Pa)	1.01 ± 0.46	0.94 ± 0.35	0.12	0.60 ± 0.08	0.66 ± 0.09	0.13	1.03 ± 0.53	0.97 ± 0.39	0.47	0.95 ± 0.22	0.83 ± 0.23	0.13
Inner dist AAo WSS (Pa)	0.96 ± 0.27	1.01 ± 0.28	0.33	0.73 ± 0.08	0.76 ± 0.14	0.88	0.97 ± 0.29	0.96 ± 0.29	0.64	0.94 ± 0.23	1.13 ± 0.33	0.13
Outer dist AAo WSS (Pa)	1.26 ± 0.54	1.27 ± 44	1.00	0.66 ± 0.20	0.80 ± 0.18	0.13	1.25 ± 0.62	1.27 ± 0.51	0.92	1.28 ± 0.21	1.27 ± 0.18	1.00
Average AAo WSS (4 regions) (Pa)	1.04 ± 0.31	1.04 ± 0.26	0.81	0.67 ± 0.10	0.73 ± 0.12	0.13	1.04 ± 0.35	1.04 ± 0.28	0.92	1.04 ± 0.18	1.06 ± 0.22	0.63

A *P* value <0.05 was considered statistically significant. All significant values are in bold

AAo ascending aorta, *DAo* descending aorta, *dist* distal, *F* female, *M* male, *prox* proximal, *WSS* wall shear stress

Table 3

Correlations among hemodynamic parameters, z-scores and age

Correlation	Pearson's r	*P* value
Aortic root Δ z-score with baseline AAo WSS	0.01	0.95
Aortic root Δ z-score with baseline AAo peak velocity	0.36	0.13
Aortic root Δ z-score/year with baseline AAo WSS	−0.07	0.78
Aortic root Δ z-score/year with baseline AAo peak velocity	0.32	0.18
AAo Δ z-score with baseline AAo WSS	0.31	0.21
AAo Δ z-score with baseline AAo peak velocity	**0.57**	**0.01**
AAo Δ z-score/year with baseline AAo WSS	0.29	0.24
AAo Δ z-score/year with baseline AAo peak velocity	**0.58**	**0.01**
AAo Δ WSS with baseline age	0.12	0.64
AAo Δ peak velocity with baseline age	0.1	0.67
AAo baseline WSS with AAo diameter/BSA	−0.25	0.32

A *P* value <0.05 was considered statistically significant. All significant values are in bold

AAo ascending aorta, *BSA* body surface area, *WSS* averaged wall shear stress over all aortic regions of interest